

## FABRICATION OF SODIUM ALGINATE/GUM GHATTI IPN MICROBEADS INTERCALATED WITH KAOLIN NANO CLAY FOR CONTROLLED RELEASE OF CURCUMIN

D. GANESH<sup>1</sup>, P. SURESH<sup>2</sup>, G. SRINIVAS RAO<sup>1\*</sup>

<sup>1</sup>Department of Chemistry, GIS, GITAM (Deemed to be University), Visakhapatnam 530045, Andhra Pradesh, India, <sup>2</sup>Department of Chemistry, SCNR Government Degree College, Proddatur, Kadapa 516360, Andhra Pradesh, India  
Email: [sgolagan@gitam.edu](mailto:sgolagan@gitam.edu)

Received: 09 Oct 2020, Revised and Accepted: 12 Dec 2020

### ABSTRACT

**Objective:** The objective of this study is to fabricate sodium alginate (SA)/gum ghatti (GG) microbeads intercalated with Kaolin (KA) nano clay for the sustained release of curcumin (CUR).

**Methods:** The microbeads were prepared by a simple ionotropic gelation technique. The developed beads were characterized by fourier transform infrared spectroscopy (FTIR), differential scanning calorimetry (DSC), thermogravimetric analysis (TGA), X-ray diffraction (X-RD), and scanning electron microscopy (SEM). Swelling studies and *in vitro* release studies were investigated under both pH 7.4 and pH 1.2 at 37 °C.

**Results:** The developed microbeads were characterized by FTIR, which confirms the interaction between CUR, polymeric matrix and KA. DSC and XRD analysis reveals that the CUR has molecularly dispersed in the polymer matrix. *In vitro* results illustrated that microbeads were influenced by the pH of test media, which might be suitable for intestinal drug delivery. The drug release mechanism was analyzed by fitting the release data into different kinetic equations and n values are obtained in the range of 0.609-0.640, suggesting that the developed microbeads showed the non-Fickian diffusion type drug release.

**Conclusion:** These results clearly illustrated that the developed KA intercalated polymeric microbeads are potential drug carriers for the controlled release of CUR.

**Keywords:** Gum Ghatti, Kaolin, Sodium alginate, Curcumin, Microbeads

© 2021 The Authors. Published by Innovare Academic Sciences Pvt Ltd. This is an open access article under the CC BY license (<http://creativecommons.org/licenses/by/4.0/>)  
DOI: <http://dx.doi.org/10.22159/ijap.2021v13i1.39963>. Journal homepage: <https://innovareacademics.in/journals/index.php/ijap>

### INTRODUCTION

In today's pharmaceutical formulations, polymers play a vital role in the progression of drug delivery technology by offering different types of pharmaceutical dosage formulations such as oral, parenteral, semisolid, controlled and sustained drug delivery systems because it can control the drug release and also it may increase the safety, efficacy, and bioavailability of the drugs with increased patient compliance [1-3]. Over the past few decades, polymeric interpenetrating polymer network (IPN) hydrogel microbeads have been broadly used as an intelligent biomaterial in many biomedical applications such as drug delivery and tissue engineering due to their excellent physical and chemical properties such as high water absorption tendency, high mechanical strength, capable of swelling under physiological conditions, providing a suitable environment for cell adhesion and new bone formation [4-6]. However, hydrogels have few disadvantages such as unconstrained release rate and uncontrolled swelling properties, leading to several side effects. To overcome these problems, certain substances have been introduced into the hydrogels such as clay minerals, surface coating with other polymers such as poly-L-Lysine [7], chitosan [8]. By introducing clay minerals such as Kaolin, montmorillonite into hydrogels, this controls the release rate of hydrogels, minimizing side effects and maintaining the drug concentration at effective levels in plasma over a period of time [9].

During the last few years, a wide range of clay minerals have been used in pharmaceutical and biomedical fields exclusively for controlled drug delivery systems because it can control the efficiency and consistency in dosage formulations and also improve the bioavailability of the drug molecules due to their larger specific surface area and considerable ion-exchange capacity which attributes to their ability to control the efficiency of bioactive molecules [10-12]. Kaolin is a hydrated two-dimensional (2D) aluminosilicate clay mineral which has been extensively used in biomedical related applications such as an activating agent for blood clotting [13], as an ingredient for operation hemostasis [14] and also

used in drug delivery systems for prolonged-release, especially of basic drugs because it can act as an active excipient in pharmaceutical dosage forms to increase the efficiency and bioavailability of drug molecules [15]. In fact their medicinal utilities have been discovered by many traditional civilizations (Egyptians, Assyrians, Babylonians, Indians, Chinese), Greeks, Romans and medieval Arab Muslims till the recent times [16].

Curcumin is a yellow bioactive compound obtained from the yellow spice of *Curcuma longa*, possesses a wide variety of pharmacological properties such as antibacterial, antioxidant, anti-inflammatory, anti-malarial, antifungal antiviral and also enhances anti-tumor activity against different types of cancer cells, including colon, prostate and breast cancers [17-19]. Due to its poor solubility and rapid metabolism, its biomedical applications are limited which results in poor bioavailability [20]. To increase the bioavailability and encapsulation efficiency of CUR, KA clay mineral was used in the present study because KA intercalates with drug molecules by adsorption process, which in turn increases the encapsulation and bioavailability of CUR.

Gum Ghatti (GG) is an anionic polysaccharide obtained from the species *Anogeissus latifolia*, comprising of linked -D-galactopyranose major units and alternating 4-O-substituted and 2-O-substituted-d-mannopyranose units along with a single L-arabinofuranose unit as side chain [21, 22]. GG has widely used in food and pharmaceutical applications, due to its excellent emulsification property, many researchers have shown potential interest in the usage of GG in drug delivery applications as a controlling polymer [23]. Sodium alginate (SA) is a linear anionic polymer consisting of various amounts of 1-4 linked  $\beta$ -D-guluronic acid and  $\alpha$ -L-mannuronic acid residues. SA has been commonly used in the food and biomedical applications due to its flexible characters such as biocompatible, biodegradable, inherent hydrophilicity and non-toxic in nature [24]. SA forms three dimensional hydrogel networks through the electrostatic attraction between carboxylic acid groups of guluronic acid residues and divalent ions ( $\text{Ca}^{2+}$ ,  $\text{Mg}^{2+}$  and  $\text{Ba}^{2+}$ ) and makes egg-box structure [25]. However, the SA

hydrogels have few limitations such as uncontrolled swelling properties and drug release profiles [26]. To overcome these limitations the SA polymer is blended with other polymers, grafting with monomers and incorporation of clay minerals [9].

In the present research work, we focussed on the fabrication of SA/GG microbeads intercalated with KA. The incorporation of KA in the polymer matrix increases the bioavailability of CUR and also controls the release rate of CUR. The developed microbeads were characterized by different techniques such as FTIR, DSC, TGA, X-RD and SEM. The swelling studies and *in vitro* drug release kinetics were performed in both simulated intestinal fluid and simulated gastric fluid at 37 °C and the results are presented here.

## MATERIALS AND METHODS

### Materials

Gum Ghatti and Kaolin were purchased from Sigma Aldrich (USA). Sodium alginate and calcium chloride were purchased from Sd. Fine chemicals, Mumbai, India. Curcumin was purchased from Loba Chemicals, Mumbai, India. Millipore water was used throughout the study.

## Methods

### Synthesis of SA/GG/KA microbeads

CUR encapsulated SA/GG/KA microbeads were prepared by simple gelation technique [27]. SA and GG aqueous dispersions about 2% of each were prepared separately using millipore water. The blends of SA and GG were prepared by mixing varying amounts (i.e. 80:20, 60:40, and 40:60) in double distilled water and stirred well to form homogeneous mixture. To this blend mixture, different amounts of KA (as per given table 1) was added and stirred well up to formation of homogeneous mixture. Then required amounts of CUR was added and stirred to obtain a homogeneous solution. Afterwards the suspension was placed in sonicator for 5 min to get homogenous suspension. The resulting solution was added drop wise in to 5 % CaCl<sub>2</sub> solution, where the spherical beads formed instantly were kept for 30 min. The obtained wet beads were collected by decantation, washed three times with double distilled water to remove the drug attached on the bead surface, and finally were dried in air overnight at room temperature. A schematic diagram (fig. 1) for the preparation procedure is given below.

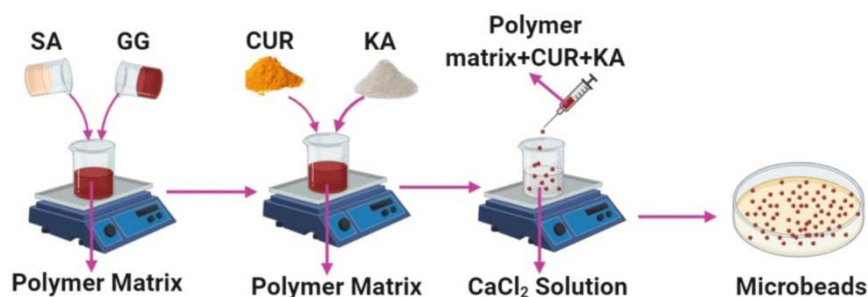


Fig. 1: Schematic procedure for the preparation of CUR loaded SA/GG/KA microbeads

Table 1: Formulation and composition of all samples

Formulation code	SA (w/v)	GG (w/v)	KA	Drug (mg)
SG1	80	20	100	100
SG2	70	30	100	100
SG3	60	40	100	100
SG4	60	40	200	100
SG5	60	40	300	100
SG6	60	40	100	150
SG7	60	40	100	200
Placebo	60	40	00	000

## Characterizations methods

### Intercalation kinetics

To estimate the maximum time required for intercalation of CUR with KA, 25 mg of CUR and 50 mg of KA was weighed and dissolved in 10 ml of double distilled water with continuous stirring at 37 °C. At regular intervals of time (15, 30, 60, 90, 120, 240 and 360 min) the drug solution was filtered and concentration of CUR was assayed using UV spectrophotometer at fixed  $\lambda_{max}$  value of 470.00 nm.

### Fourier transform infrared spectral analysis

Fourier transform infrared spectroscopy (FTIR) spectra of SA, GG, CUR, KA, placebo microbeads, and drug loaded microbeads were recorded with FTIR spectrophotometer (model Bomem MB-3000, with Horizon MB™ FTIR software) in the wavelength range of 400–4000 cm<sup>-1</sup> to find out the possible chemical interactions between polymers and drug.

### Differential scanning calorimetry (DSC)

DSC curves of SA, GG, CUR, KA, Placebo microbeads, and drug loaded microbeads were recorded using Thermogravimetry analyzer (Rheometric Scientific, Model DSC-SP, UK). The analysis was

performed by heating the sample from 40 to 600 °C at a heating rate of 10 °C/min under nitrogen atmosphere.

### Thermogravimetric analysis (TGA)

Thermogravimetric analysis of SA, GG, CUR, KA, Placebo microbeads, and drug loaded microbeads were carried out using Thermogravimetry analyzer Rheometric Scientific, Model DSC-SP, UK. About 5-7 mg of sample was placed into alumina crucible and the thermo grams were recorded between 40 °C to 600 °C at a heating rate of 10 °C/min under nitrogen atmosphere.

### X-ray diffraction (XRD)

The X-ray diffraction of CUR, placebo microbeads, and drug loaded microbeads were performed by a wide angle X-ray scattering diffractometer (Panalytical X-ray Diffractometer, model-X'pert Pro) with CuK $\alpha$  radiation ( $\lambda = 1.54060$ ) at a scanning rate of 10 °/min to determine the crystallinity.

### Scanning electron microscopy (SEM)

The morphological characterization of microbeads was observed by using SEM (JOEL MODEL JSM 840A) with an accelerated voltage of 20 kV.

### Encapsulation efficiency

A known mass of drug loaded microbeads (20 mg) were immersed into 100 ml of phosphate buffer solution (pH 7.4 containing 5 % absolute ethyl alcohol) for 24 h and then vigorously stirred the microbeads to ensure the complete extraction of CUR from the microbeads. Supernatants were filtered and analyzed by ultraviolet (UV) spectrophotometer (LabIndia, Mumbai, India) at the  $\lambda_{\max}$  of 470.00 nm with placebo microbeads were used as a blank correction. Concentration of drug was determined by using calibration curve constructed by series of CUR standard solutions. Percentage of encapsulation efficiency was determined by the following formula.

$$\% \text{ EE} = \frac{\text{CUR initially added (mg)} - \text{Free CUR (mg)}}{\text{CUR initially added (mg)}} \times 100$$

### Swelling measurements

The swelling behaviour of different formulations was determined gravimetrically in simulated intestinal fluid (pH 7.4) and simulated gastric fluid (pH 1.2) at 37 °C. The % of equilibrium swelling degree was calculated using the following equation:

$$\% \text{ swelling degree} = \frac{W_s - W_d}{W_d} \times 100$$

Where  $W_s$  is the weight of swollen beads and  $W_d$  is the weight of dry beads.

### In vitro drug release studies

*In vitro* drug release studies of different formulations were carried out by using a dissolution tester (Lab India, Mumbai, India) containing eight baskets each with 900 ml of phosphate buffer solution (PBS) maintained at 37 °C, at a rotation speed of 50 rpm to replicate intestinal fluid (pH 7.4) and gastric fluid (pH 1.2) atmosphere respectively. 100 mg of the CUR loaded microbeads were taken in a dialysis bags for the drug release studies. At regular intervals of time, 5 ml aliquot samples were withdrawn, and analyzed using UV spectrophotometer at fixed  $\lambda_{\max}$  value of 470.00 nm, and the released drug amount was obtained by using concentration versus absorbance calibration curves. The withdrawn aliquot samples were replenished with equal volumes of PBS to stimulate physiological conditions. The sink conditions were maintained throughout the release study.

### Drug release kinetics

The drug release kinetics was analyzed by fitting the data in to kinetic models, which include zeroth, first order, Higuchi and

Korsmeyer-Peppas [28-31]. Based on the goodness of data fit, the most suitable model was also determined [32].

## RESULTS AND DISCUSSION

### Intercalation kinetics

From fig. 2, it was observed that 14.51 % of CUR was intercalated with KA electrostatically within 90 min and remained constant up to 360 min. So, in the following experiments, we will keep 90 min time for interaction between CUR and KA to prevent partial interaction.

### FTIR spectral analysis

The FTIR spectra of GG, SA, KA, CUR, placebo microbeads and drug loaded microbeads (SG7) are represented in fig. 3. The FTIR spectra of CUR shows a characteristic broad peak at 3496  $\text{cm}^{-1}$ , which corresponds to phenolic O-H stretching vibrations, a peak at 2923  $\text{cm}^{-1}$  is assigned to aromatic C-H stretching vibrations, a peak at 1596  $\text{cm}^{-1}$  corresponds to the stretching vibration of benzene ring skeleton, a peak at 1513  $\text{cm}^{-1}$  corresponds to mixed (C=O) and (C=C) vibration, a peak at 1272  $\text{cm}^{-1}$  is assigned to Ar-O stretching vibrations [20]. The FTIR spectra of KA shows characteristic peaks at 3688 and 3625  $\text{cm}^{-1}$  corresponds to O-H stretching frequency of Si-OH and Al-OH respectively, a peak at 3456  $\text{cm}^{-1}$  assigned to H-O-H stretching frequency of interlayer water, peak at 2360  $\text{cm}^{-1}$  was attributed to C-H stretching frequency, peak at 1596  $\text{cm}^{-1}$  corresponds to O-H adsorbed water, the absorption peaks at 1126 and 902  $\text{cm}^{-1}$  corresponds to Si-O-Si stretching peak [33]. FTIR spectra of SA shows a peak at 3417  $\text{cm}^{-1}$  is responsible for O-H stretching vibrations, a peak at 1596  $\text{cm}^{-1}$  is assigned to C=O stretching vibrations, a peak at 1383  $\text{cm}^{-1}$  corresponds to COO-asymmetric stretching frequency. On comparing the FTIR spectra of placebo microbeads and drug loaded microbeads (SG7), a new peak at 1510  $\text{cm}^{-1}$  was observed, which similar to that of C=C stretching vibration of CUR, suggesting that drug was present in SG7. And also the peak at 1595  $\text{cm}^{-1}$  in placebo microbeads was shifted to 1592  $\text{cm}^{-1}$  in drug loaded SG7 microbeads, which confirmed that the drug interacts with the polymer matrix. In the case of SG7, the O-H stretching frequency was decreased due to the interaction of KA with active sites of polymer molecules and also a new peak appears at 910  $\text{cm}^{-1}$ , which confirmed that the KA intercalates with active sites of polymer matrices and drug molecules [34].

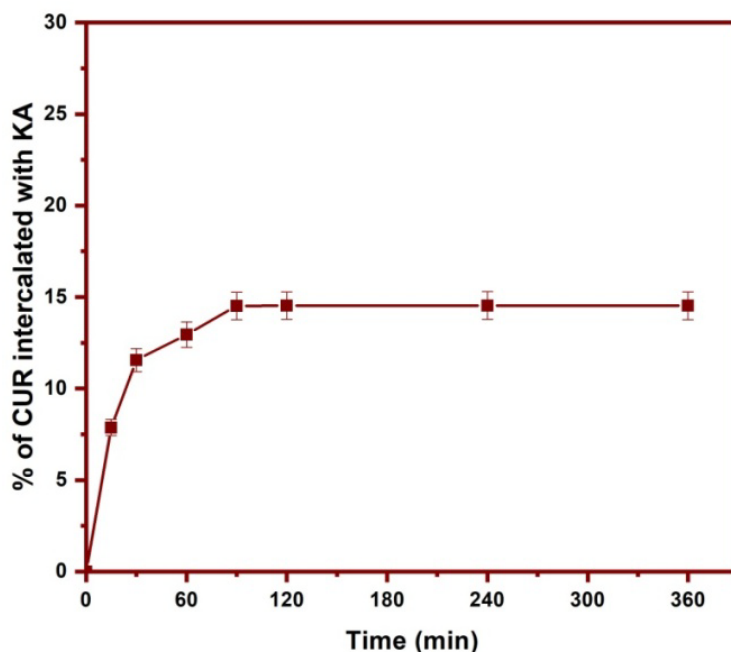


Fig. 2: Effect of time for intercalation of CUR with KA

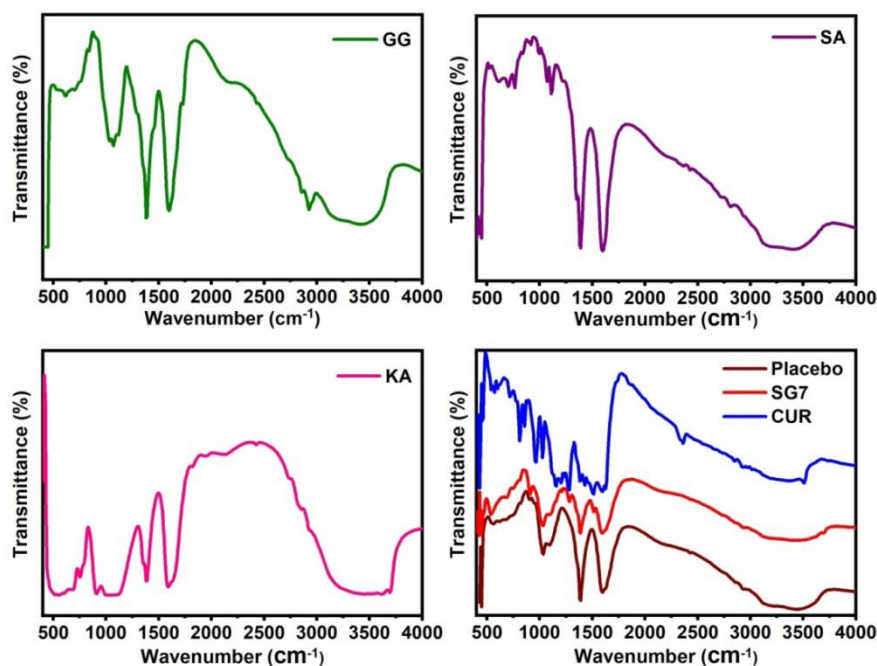


Fig. 3: FTIR spectrum of GG, SA, KA, CUR, placebo microbeads, and drug loaded SA/KA microbeads (SG7)

### Thermal analysis

To investigate the interaction of polymer matrix with KA as well as the crystalline nature of encapsulated CUR in the polymer matrix, DSC analysis was performed and the DSC curves were displayed in fig. 4. The thermogram of KA shows a peak at 272 and 496 °C, whereas SG7 microbeads also showed similar peaks like that of KA at 331 and 578 °C but a slight variation was observed, which confirmed that the interaction takes place between active sites of the polymer matrix and KA [15]. The peaks in SG7 were shifted to the higher side due to the interaction between the polymer matrix and KA. DSC curve of CUR shows a sharp peak at 189 °C, whereas such a peak was not observed in SG7 microbeads, which confirmed that the drug was molecularly dispersed in the microbeads [35]. To estimate the thermal stability of developed microbeads TGA analysis was performed and the results are displayed in fig. 4. The TGA curve of GG showed two weight loss steps, the first weight loss step was observed between the regions of 40-162 °C with weight loss of 7%, which is due to the evaporation of water molecules adsorbed on the surface. The second weight loss step with a weight loss of 67% was found in the region of 165-600 °C, which corresponds to the degradation of GG polymer. The thermal decomposition of SA occurs in three consecutive steps. The first weight loss step with weight loss of 17 % was observed in the region of 40-116 °C due to the dehydration process. The next step was observed in the region of 121-214 °C with a loss of 4% followed by the third step with weight loss of 48 % in between the region of 225-600 °C, which is due to the formation of sodium carbonate residue [36]. The TGA curve of CUR showed that the CUR should remain stable up to 168 °C, after that it follows mass loss and being maximum at 391 °C due to total degradation of the compound. In the case of KA, weight loss of 6 % was observed between 40 to 256 °C corresponds to the dehydration of water molecules adsorbed in pores and between the silicate layers and followed by weight loss of 13% in between the region of 258-600 °C, corresponds to the loss of structural water. The TGA curve of placebo microbeads showed three weight loss steps. The first weight loss step was found between 40-181 °C with a loss of 22 %, which is due to the dehydration of adsorbed water. The next two steps were observed in the region of 192-295 °C and 305-600 °C with a weight loss of 24 % and 31 %, which indicates the decomposition of the polymer network. In the case of drug loaded microbeads (SG7) three weight loss steps were observed. The first weight loss of 12 % was observed in the region of 42-191 °C, which is ascribed to the evaporation of water molecules adsorbed on the surface of

microbeads. The second step was observed in the region of 197-313 °C with a loss of 20 %, followed by weight loss of 18 % in between the region of 321-600 °C, which corresponds to the decomposition of the polymer network. The TGA results suggest that the developed microbeads show an overall improvement in thermal stability.

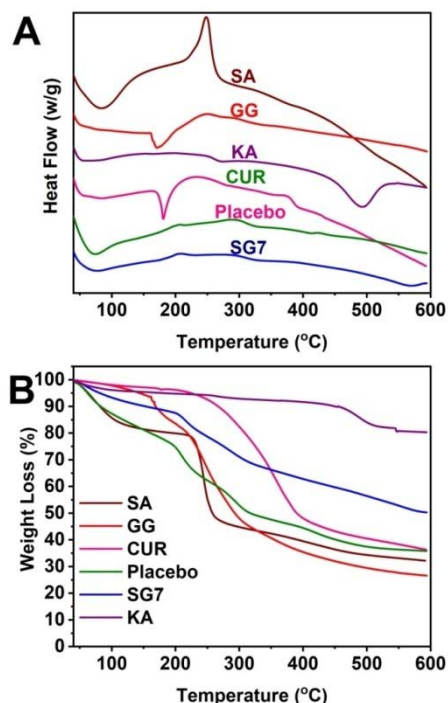


Fig. 4: Thermal analysis (A) DSC and (B) TGA

### X-RD analysis

XRD analysis was performed to find out the molecular dispersion of CUR in the polymer matrix and the presence of KA in the microbeads. The diffractograms of CUR, KA, placebo and SG-7

microbeads were presented in fig. 5. The XRD pattern of CUR showed various  $2\theta$  peaks in between 12-28°, which is due to the crystalline nature of CUR. Whereas in SG-7 these peaks were not observed, suggesting that CUR crystalline peaks were merged with the polymer matrix, which indicates that the CUR changes its state from crystalline to amorphous nature. These results suggesting that the CUR has molecularly dispersed in the polymeric matrix. The XRD

pattern of KA shows characteristic peaks at 11.95°, 18.34°, 19.97° and 24.84° which is due to the presence of kaolinite, the multiple reflection peak at 26.6° indicates the presence of quartz in kaolin clay. A similar observation was observed by Dewi *et al.* [37] from their characterization analysis of Kaolin. Similar peaks of KA were observed in the SG-7 microbeads, which indicate the presence of KA in the microbeads.

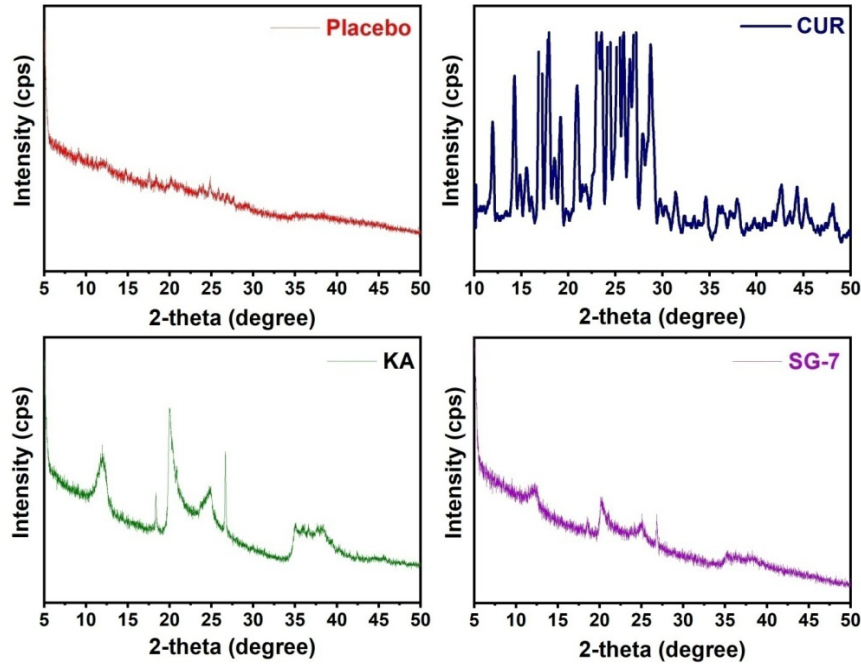


Fig. 5: XRD patterns of placebo, CUR, KA and SG-7 microbeads

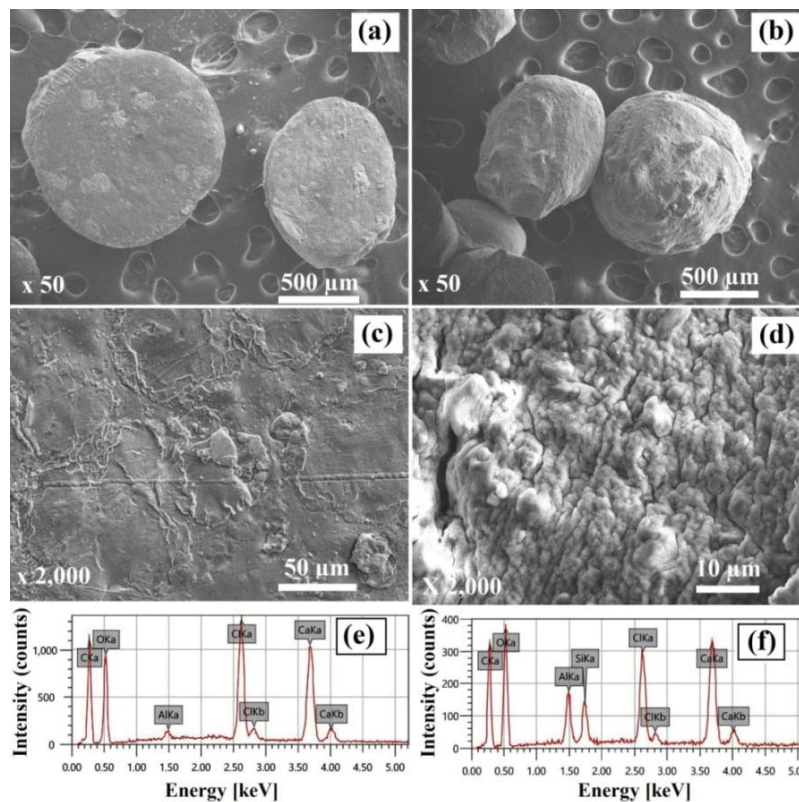


Fig. 6: SEM images of placebo microbeads (a,c) and SG7 microbeads (b,d); EDS analysis of placebo microbeads (e) and SG7 microbeads (f)

### SEM and energy-dispersive X-ray spectra (EDS) analysis

To examine the morphological structure in the developed microbeads SEM analysis was performed and the results were displayed in fig. 6. As shown in the fig. 6, the microbeads are spherical having rough surfaces. On comparing the placebo microbeads (fig. 6a and 6c) the surface of SG-7 (fig. 6b and 6d) shows higher roughness, which is due to the presence of KA platelets on the surface of microbeads, this confirms the presence of KA in the microbeads. From the results of SEM images, the average size of microbeads was found to be 800–1500  $\mu\text{m}$ .

To investigate the elements in the microbeads EDS analysis was performed and the results are presented in fig. 6. The EDS spectra of placebo microbeads (fig. 6e) showed C, O, Al, Cl and Ca elemental peaks. Similar peaks were observed in SG-7 (fig. 6f), along with that Na, Al and Si peaks were observed, which confirms the presence of KA in the microbeads. These results are in good agreement with Reddy *et al.* [15] who found similar peaks of KA from their sodium alginate/gelatin microbeads-intercalated with kaolin nanoclay for controlled release of D-Penicillamine.

### Swelling measurements

Swelling degree is one of the main factors of polymeric microbeads in drug delivery systems for the controlled release of drugs. Swelling degree experiments were carried out at pH 1.2 and 7.4 at 37 °C and the results were presented in fig. 7. The swelling degree results reveal that a higher swelling degree was observed at pH 7.4 than at pH 1.2 because at pH 7.4 the carboxylic groups became ionized into COO<sup>-</sup>ions, which results electrostatic repulsion between COO<sup>-</sup>groups caused the microbeads to swell. A similar observation was reported by Reddy *et al.* [6] from their smart karaya gum/sodium alginate semi-IPN microbeads. Hence, the developed microbeads are good promising carriers to deliver drug molecules at the intestine and to avoid gastric release of drugs.

### Encapsulation efficiency (% EE)

The percentage of encapsulation efficiency from drug encapsulation studies was found to be between 43 % and 54 % (table 2). The % EE of CUR depends on different parameters such as % of blend composition, the extent of drug loading and the amount of KA. The %

EE increased with the increase of SA content in the blend matrix, with increase the % of SA in blend composition, CUR-SA interactions increases consequently % EE increased [38]. As the % of drug loading is increased, % EE also increased this may be due to higher drug concentration, which causes entrapment of more drug molecules in the polymeric matrix leading to higher % EE. As the amount of KA increases in the polymer matrix, the % EE increased this is due to the formation of hydrogen bonding between free-OH groups of KA and CUR.

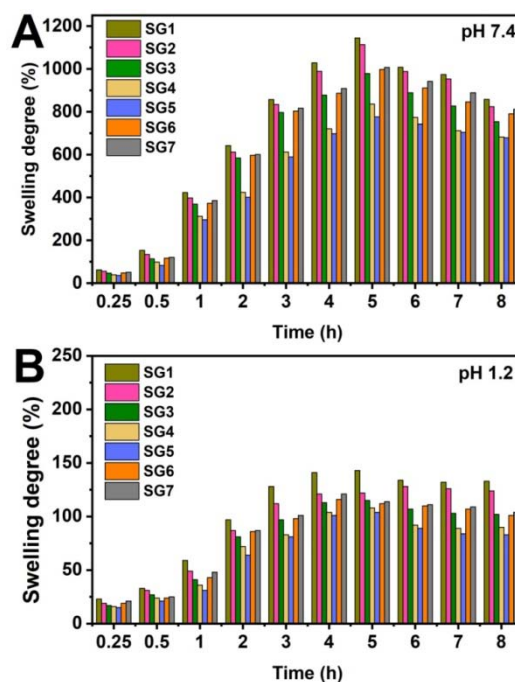


Fig. 7: Swelling studies of Ca, CaMg, CaBa and CaAl at pH 7.4 and pH 1.2 at 37 °C

Table 2: Encapsulation efficiency (% EE) of all samples

S. No.	Formulation code	%EE
1	SG1	47 ± 0.8
2	SG2	45 ± 1.9
3	SG3	43 ± 1.6
4	SG4	52 ± 1.1
5	SG5	54 ± 1.5
6	SG6	46 ± 1.3
7	SG7	47 ± 1.2

(Results are expressed as mean ± SD, n=3)

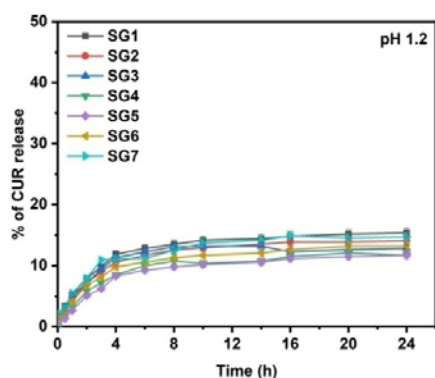


Fig. 8: *In vitro* release profiles of CUR microbeads at 37 °C in pH 1.2

### *In vitro* drug release studies

The *in vitro* CUR release studies of all formulations were investigated under both pH 1.2 and pH 7.4 at 37 °C and the results are displayed in fig. 8-11. The results reveal that the percentage of CUR release is higher in pH 7.4 rather than pH 1.2, which is due to a higher pH (7.4) the carboxylate group shows less interactions with the buffer media, hence the network becomes slacker, therefore the entrapped drug molecules leached out easily from the polymer matrix. *In vitro* drug release studies for all formulations at pH 7.4 were discussed in terms of polymer blend variation, drug variation, and KA variation, and the results are displayed in fig. 9 to 11.

### Effect of polymer content

To find out the impact of polymer blend composition on % release of CUR was studied at a constant amount of CUR (100 mg) and KA (100 mg). The formulations SG1, SG2 and SG3 have different polymer compositions and their drug release results are displayed in fig. 9. The results suggested SG1 showed a higher release rate than the SG2 and SG3, this is due to SA content increases in the polymer matrix,

and swelling of the polymer matrix also increases due to the hydrophilic nature of SA. A similar observation was reported by Madhavi et al. [27] from their drug delivery studies of sodium alginate–locust bean gum IPN hydrogel beads.

The formulation SG7 showed a higher drug release rate than SG6 and SG3. Thus the release rates vary depending upon the amount of drug present in the matrices i.e. release is higher for those formulations having a higher amount of drug and vice-versa.

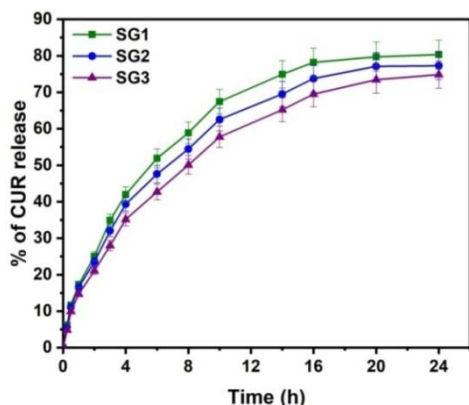


Fig. 9: Effect of polymer blend composition on % of CUR release at 37 °C in pH7.4

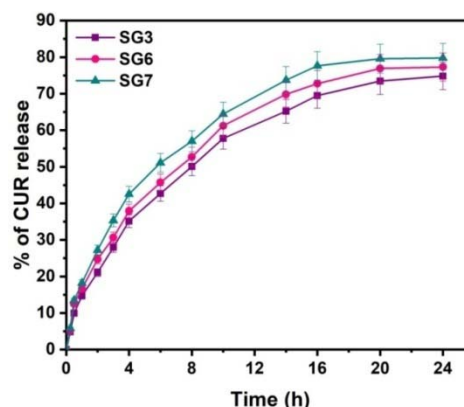


Fig. 11: Effect of drug content on % of CUR release at 37 °C in pH7.4

**Effect of KA content**

The effect of KA on the release rate of CUR was investigated by varying the extent of KA and the results are displayed in fig. 10. The release rate of SG3 (100 mg), SG4 (200 mg) and SG5 (300 mg) are 74, 72 and 68 % respectively are displayed in fig. 10. The results suggested that the amount of KA increases, the drug release rate decreases. This is because the intercalated drug cannot be exchanged completely with phosphate ions in the buffer solution during the ion exchange process, which results incomplete release process.

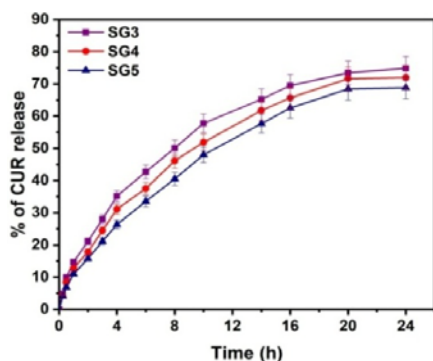


Fig. 10: Effect of KA content on % of CUR release at 37 °C in pH7.4

**Effect of drug content**

To find out the effect of drug loading on *in vitro* release profiles was studied at a constant amount of polymer blend composition and KA. The formulations SG3, SG6 and SG7 have different drug concentrations and their drug release results are displayed in fig. 11.

**Drug release kinetics**

The obtained *in vitro* drug release data of CUR loaded microbeads at pH 7.4 were fitted into different mathematical models such as zero order, first order and Higuchi. The release rate constant and correlation coefficient of all formulations are shown in table 3 and fig. 12. The correlation coefficient values of CUR loaded microbeads neither follows zero order nor first order, but the correlation coefficient values were close to the Higuchi model. Therefore, the drug release kinetics of CUR loaded microbeads follows Higuchi model. According to Higuchi model the release of drug from the microbeads, involves the penetration of liquid into the matrix and dissolves the drug, which then diffuses the drug into the exterior liquid through pores or intestinal channels. However, this type of phenomenon is observed in hydrophilic matrix system. Therefore the drug release rate of CUR loaded microbeads show the phenomenon of swelling and erosion of the polymer simultaneously. To understand the drug release mechanism, the data obtained from *in vitro* drug release studies in PBS (7.4) were fitted into the following Korsmeyer-Peppas equation.

$$\frac{M_t}{M_\infty} = kt^n$$

Where,  $M_t$  is the cumulative release of CUR at time  $t$ ,  $M_\infty$  is the total amount of CUR in the matrix,  $k$  is a characteristic release constant of the drug-polymer system and  $n$  is the release exponent indicating the type of drug release mechanism. The results  $n$  and  $k$  are listed in table 2. For spherical drug carriers, if  $n < 0.43$ , the drug diffuses from the polymer matrix according to Fickian diffusion; if  $0.43 < n < 0.85$ , anomalous or non-Fickian type drug diffusion occurs; if  $n = 0.85$ , Case-II kinetics is operative; if  $n > 0.85$ , the mode of drug release follows the super Case-II diffusion. In the present data  $n$  values are obtained in the range of 0.609-0.640 indicates non-Fickian type of diffusion process.

Table 3: Release kinetics parameters at pH-7.4 and encapsulation efficiency (% EE) of all samples

Formulation code	Korsmeyer-peppas		Higuchi		First		Zero	
	r <sup>2</sup>	n	r <sup>2</sup>	k	r <sup>2</sup>	k	r <sup>2</sup>	k
SG1	0.990	0.625	0.957	18.378	0.936	0.0723	0.823	3.165
SG2	0.986	0.628	0.970	17.565	0.941	0.0659	0.849	3.048
SG3	0.984	0.640	0.981	17.029	0.947	0.0614	0.877	2.984
SG4	0.972	0.638	0.988	16.677	0.945	0.0574	0.906	2.955
SG5	0.962	0.609	0.990	16.137	0.956	0.0522	0.927	2.887
SG6	0.981	0.634	0.976	17.405	0.947	0.0658	0.865	3.038
SG7	0.983	0.625	0.964	17.852	0.949	0.0705	0.835	3.084

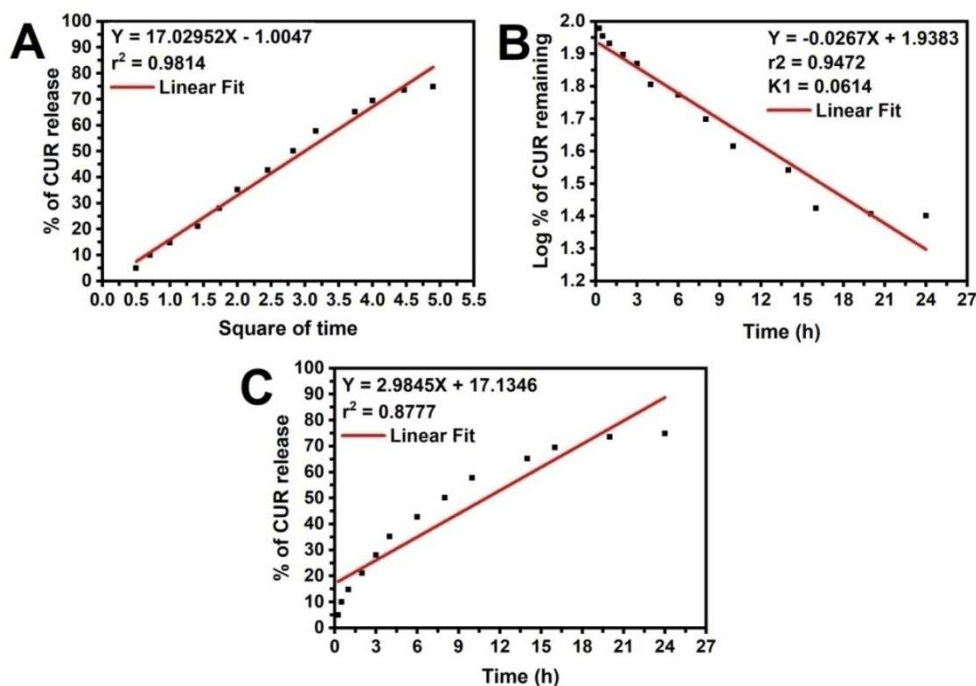


Fig. 12: Evaluation of drug release models in PBS 7.4 at 37 °C (A) Higuchi model (B) first order and (C) zero order

## CONCLUSION

In the present study, semi-IPN microbeads were fabricated from SA/GG intercalated with KA by a simple ionotropic technique. Microbeads formation was confirmed by FTIR spectroscopy. DSC and X-RD confirm the molecular level dispersion of CUR into microbeads. Morphological studies reveal that the microbeads were spherical in shape with a rough surface. From the SEM studies, the average diameter of microbeads was found to be 800–1500  $\mu\text{m}$ . Results of the swelling and *in vitro* release studies confirm that the fabricated microbeads are suitable for interstitial drug delivery. *In vitro* releases studies fitted into the Peppas equation and followed the non-Fickian diffusion transport. Based on the results, it was suggesting that the developed microbeads were potentially good carriers for the controlled release of CUR.

## FUNDING

Nil

## AUTHORS CONTRIBUTIONS

All the author has contributed equally.

## CONFLICTS OF INTERESTS

Declared none

## REFERENCES

- Ganguly S, Maity PP, Mondal S, Das P, Bhawal P, Dhara S, et al. Polysaccharide and poly(methacrylic acid) based biodegradable elastomeric biocompatible semi-IPN hydrogel for controlled drug delivery. *Mater Sci Eng C* 2018;92:34-51.
- Reddy OS, Subha M, Jithendra T, Madhavi C, Rao KC. Fabrication of Gelatin/Karaya gum blend microspheres for the controlled release of distigmine bromide. *J Drug Delivery Ther* 2019;9:1-11.
- Liechty WB, Kryscio DR, Slaughter BV, Peppas NA. Polymers for drug delivery systems. *Annu Rev Chem Biomol Eng* 2010;1:149-73.
- Peppas N, Bures P, Leobandung W, Ichikawa H. Hydrogels in pharmaceutical formulations. *Eur J Pharm Biopharm* 2000;50:27-46.
- George A, Shah PA, Shrivastav PS. Natural biodegradable polymers based nano-formulations for drug delivery: a review. *Int J Pharm* 2019;561:244-64.
- Reddy OS, Subha M, Jithendra T, Madhavi C, Rao KC. Fabrication and characterization of smart karaya gum/sodium alginate semi-IPN microbeads for controlled release of D-penicillamine drug. *Polym Polym Compos* 2020. <https://doi.org/10.1177/0967391120904477>.
- Constantinidis I, Grant SC, Celper S, Gauffin Holmberg I, Agering K, Oca Cossio JA, et al. Non-invasive evaluation of alginate/poly-L-lysine/alginate microcapsules by magnetic resonance microscopy. *Biomaterials* 2007;28:2438-45.
- Jithendra T, Reddy OS, Subha M, Madhavi C, Rao KC. Xanthan gum graft copolymer/sodium alginate micro beads coated with chitosan for controlled release of chlorthalidone drug. *Int J Pharm Sci Res* 2020;11:1132-45.
- Reddy OS, Subha MCS, Jithendra T, Madhavi C, Rao KC. Curcumin encapsulated dual cross linked sodium alginate/montmorillonite polymeric composite beads for controlled drug delivery. *J Pharm Anal* 2020. DOI:10.1016/j.jpha.2020.07.002
- Zhang W, Ding Y, Boyd SA, Teppen BJ, Li H. Sorption and desorption of carbamazepine from water by smectite clays. *Chemosphere* 2010;81:954-60.
- Massaro M, Colletti CG, Lazzara G, Riel S. The use of some clay minerals as natural resources for drug carrier applications. *J Funct Biomater* 2018;9:58.
- Carretero MI, Pozo M. Clay and non-clay minerals in the pharmaceutical industry: part I. Excipients and medical applications. *Appl Clay Sci* 2009;46:73-80.
- Liang Y, Xu C, Li G, Liu T, Liang JF, Wang X. Graphene-kaolin composite sponge for rapid and riskless hemostasis. *Colloids Surf B* 2018;169:168-75.
- Sena MJ, Douglas G, Gerlach T, Grayson JK, Pichakron KO, Zierold D. A pilot study of the use of kaolin-impregnated gauze (Combat Gauze) for packing high-grade hepatic injuries in a hypothermic coagulopathic swine model. *J Surg Res* 2013;183:704-9.
- Reddy OS, Subha M, Jithendra T, Madhavi C, Rao KC, Mallikarjuna B. Sodium alginate/gelatin microbeads-intercalated with kaolin nanoclay for emerging drug delivery in wilson's disease. *Int J Appl Pharm* 2019;11:71-80.
- Awad ME, Lopez Galindo A, Setti M, El-Rahmany MM, Iborra CV. Kaolinite in pharmaceuticals and biomedicine. *Int J Pharm* 2017;533:34-48.

17. Behbahani ES, Ghaedi M, Abbaspour M, Rostamizadeh K, Dashtian K. Curcumin loaded nanostructured lipid carriers: *in vitro* digestion and release studies. *Polyhedron* 2019;164:113-22.
18. Sun J, Bi C, Chan HM, Sun S, Zhang Q, Zheng Y. Curcumin-loaded solid lipid nanoparticles have prolonged *in vitro* antitumour activity, cellular uptake and improved *in vivo* bioavailability. *Colloids Surf B* 2013;111:367-75.
19. Chen HW, Huang HC. Effect of curcumin on cell cycle progression and apoptosis in vascular smooth muscle cells. *Br J Pharmacol* 1998;124:1029-40.
20. Reddy OS, Subha M, Jithendra T, Madhavi C, Rao KC. Emerging novel drug delivery system for control release of curcumin through sodium alginate/poly (ethylene glycol) semi IPN microbeads-intercalated with kaolin nanoclay. *J Drug Delivery Ther* 2019;9:324-33.
21. Boppana R, Krishna Mohan G, Nayak U, Mutalik S, Sa B, Kulkarni RV. Novel pH-sensitive IPNs of polyacrylamide-g-gum ghatti and sodium alginate for gastro-protective drug delivery. *Int J Biol Macromol* 2015;75:133-43.
22. Deshmukh AS, Setty CM, Badiger AM, Muralikrishna KS. Gum ghatti: a promising polysaccharide for pharmaceutical applications. *Carbohydr Polym* 2012;87:980-6.
23. Ray S, Roy G, Maiti S, Bhattacharyya UK, Sil A, Mitra R. Development of smart hydrogels of etherified gum ghatti for sustained oral delivery of ropinirole hydrochloride. *Int J Biol Macromol* 2017;103:347-54.
24. Chintha M, Obireddy SR, Areti P, Marata CSS, Kashayi CR, Rapoli JK. Sodium alginate/locust bean gum-g-methacrylic acid IPN hydrogels for "simvastatin" drug delivery. *J Dispersion Sci Technol* 2019;21:2192-2202.
25. Grant GT, Morris ER, Rees DA, Smith PJC, Thom D. Biological interactions between polysaccharides and divalent cations: the egg-box model. *FEBS Lett* 1973;32:195-8.
26. Sanchez Ballester NM, Soulaïrol I, Bataille B, Sharkawi T. Flexible heteroionic calcium-magnesium alginate beads for controlled drug release. *Carbohydr Polym* 2019;207:224-9.
27. Madhavi C, Babu PK, Maruthi Y, Parandhama A, Reddy OS, Rao K, *et al.* Sodium alginate-locust bean gum IPN hydrogel beads for the controlled delivery of nimesulide-anti-inflammatory drug. *Int J Pharm Pharm Sci* 2017;9:245-52.
28. Costa P, Lobo JMS. Modeling and comparison of dissolution profiles. *Eur J Pharm Sci* 2001;13:123-33.
29. Dash S, Murthy PN, Nath L, Chowdhury P. Kinetic modeling on drug release from controlled drug delivery systems. *Acta Pol Pharm* 2010;67:217-23.
30. Gouda R, Baishya H, Qing Z. Application of mathematical models in drug release kinetics of carbidopa and levodopa ER tablets. *J Dev Drugs* 2017;6:1-8.
31. Dozie Nwachukwu SO, Danyuo Y, Obayemi JD, Odusanya OS, Malatesta K, Soboyejo WO. Extraction and encapsulation of prodigiosin in chitosan microspheres for targeted drug delivery. *Mater Sci Eng C* 2017;71:268-78.
32. Arhewoh IM, Okhamafe AO. An overview of site-specific delivery of orally administered proteins/peptides and modelling considerations. *Int J Med Biomed Res* 2004;3:7-20.
33. Rezik SB, Gassara S, Bouaziz J, Deratani A, Baklouti S. Development and characterization of porous membranes based on kaolin/chitosan composite. *Appl Clay Sci* 2017;143:1-9.
34. Zhang Y, Long M, Huang P, Yang H, Chang S, Hu Y, *et al.* Intercalated 2D nanoclay for emerging drug delivery in cancer therapy. *Nano Res* 2017;10:2633-43.
35. Jithendra T, Reddy OS, Subha MCS, Rao KC. Fabrication of drug delivery system for control release of curcumin, intercalated with magnetite nano particles through sodium alginate/polyvinylpyrrolidone-co-vinyl acetate semi IPN microbeads. *Int J Appl Pharm* 2020;12:249-57.
36. Jain S, Datta M. Montmorillonite-alginate microspheres as a delivery vehicle for oral extended release of venlafaxine hydrochloride. *J Drug Delivery Sci Technol* 2016;33:149-56.
37. Dewi R, Agusnar H, Alfian Z. Characterization of technical kaolin using XRF, SEM, XRD, FTIR and its potentials as industrial raw materials. *J Phys Conf Ser* 2018. DOI:10.1088/1742-6596/1116/4/042010.
38. Govindaraju R, Karki R, Chandrashekarappa J, Santhanam M, Shankar AKK, Joshi HK, *et al.* Enhanced water dispersibility of curcumin encapsulated in alginate-polysorbate 80 nano particles and bioavailability in healthy human volunteers. *Pharm Nanotechnol* 2019;7:39-56.